ChemPubSoc Europe

DOI: 10.1002/cphc.201800008

CHEMPHYSCHEM Communications

Spin-Noise-Detected Two-Dimensional Nuclear Magnetic Resonance at Triple Sensitivity

Stephan J. Ginthör,[a] Kousik Chandra,[a, b] Matthias Bechmann,[a] Victor V. Rodin,[a] and Norbert Müller*[a, c]

Dedicated to Prof. Robert Glaser (Department of Chemistry, Ben-Gurion University of the Negev, IL) on the occasion of his 75th birthday.

A major breakthrough in speed and sensitivity of 2D spin-noise-detected NMR is achieved owing to a new acquisition and processing scheme called "double block usage" (DBU) that utilizes each recorded noise block in two independent cross-correlations. The mixing, evolution, and acquisition periods are repeated head-to-tail without any recovery delays and well-known building blocks of multidimensional NMR (constant-time evolution and quadrature detection in the indirect dimension as well as pulsed field gradients) provide further enhancement and artifact suppression. Modified timing of the receiver electronics eliminates spurious random excitation. We achieve a threefold sensitivity increase over the original snHMQC (spin-noise-detected heteronuclear multiple quantum correlation) experiment (K. Chandra et al., *J. Phys. Chem. Lett.* **2013**, *4*, 3853) and demonstrate the feasibility of spin-noise-detected long-range correlation.

Spin-noise-detected 2D NMR was introduced as a proof-of-concept recently.[1] It is based on the phenomenon of nuclear spin noise, which Felix Bloch predicted in 1946 as a consequence of the statistically incomplete cancellation of random fluctuations[2] in finite sized spin ensembles. Its first experimental observation had to wait until 1985,[3,4] because of the low signal amplitudes and, compared to today's standards, less sophisticated spectrometer hardware. Recent advances in the field, especially the wide availability of cryogenically cooled probes,[5] allowed the measurement of spin noise on many spectrometers and renewed the interest in this phenomenon.[6–8] Even if practical applications in spectroscopy are still very limited, the properties of spin noise seem a promising approach for addressing certain types of problems. Extensive research in one-dimensional spin noise spectroscopy gave rise to various novel application in the fields of spectroscopy and imaging.[7] Spin noise is also relevant for interference-free investigations of spin systems.[9] The ultimate promise, however, is the realization of nano-scale level (less than 10^8 spins) NMR spectroscopy, in a range where noise magnetization dominates over thermal polarization-based magnetization.[3,10] Our focus is set on spectroscopic applications for liquid samples.[1,7–9,11–13] To date, spin-noise-detected NMR spectroscopy is still in an early stage of development and will require additional hardware advances for implementation at nano-scale. However, in magnetic resonance force microscopy (MRFM) spin noise detection has become the state-of-the art.[14] Issues of other noise sources affecting NMR spin noise spectra have been resolved recently[8] and are briefly discussed in the Supporting Information.

The first reported 2D spin-noise-detected spectrum was the snHMQC (spin-noise-detected heteronuclear multiple quantum correlation) experiment,[1] which is based on the pairwise cross-correlation of noise blocks that symmetrically sandwich the mixing and evolution periods of a heteronuclear 2D experiment. The general timing diagram of a conventional radio frequency (RF) pulse-excited 2D NMR experiment is compared to the ones of spin-noise-detected 2D NMR experiments in Figure 1.

For a conventional 2D NMR experiment, as drawn in Figure 1a, the spin coherences are excited by one or more RF pulses, modulated during the evolution period, transferred in the mixing period(s) and detected during t_2. During evolution the amplitudes or phases of the coherences are modulated with a characteristic frequency, which may be a chemical shift, coupling constant or a linear combination of these.[15] In spin-noise-detected experiments, as schematically drawn in Figure 1b, no RF irradiation is applied to the detected spins (^{1}H in most cases), as both excitation and detection rely exclusively on intrinsic random spin fluctuations, which are usually called spin noise and are intrinsic to the tightly coupled system consisting of the nuclear spins and the resonance RF circuit.[8] For each repetition of the 2D pulse sequence, two input and output noise blocks are acquired and cross-correlated as de-

[a] S. J. Ginthör, Dr. K. Chandra, Dr. M. Bechmann, Dr. V. V. Rodin, Prof. Dr. N. Müller
Institute of Organic Chemistry
Johannes Kepler University Linz
Altenbergerstraße 69, 4040 Linz (Austria)
E-mail: norbert.mueller@jku.at

[b] Dr. K. Chandra
Present address: NMR Research Centre
Indian Institute of Science
Bangalore, 560012 (India)

[c] Prof. Dr. N. Müller
Faculty of Science
University of South Bohemia
Branišovská 1645/31A, 370 05 České Budějovice (Czech Republic)

Supporting Information and the ORCID identification number(s) for the author(s) of this article can be found under https://doi.org/10.1002/cphc.201800008.

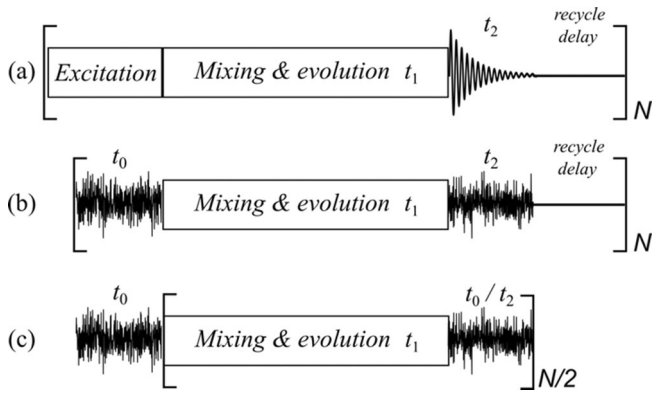

Figure 1. a) Generalized timing scheme of a pulse-excited 2D NMR experiment. t_2 denotes the acquisition block recording the FID. The period t_1 represents the indirectly detected dimension. Coherence transfer occurs during excitation and mixing periods. b) Acquisition scheme of a spin-noise-detected 2D NMR experiment. t_0 and t_2 both denote acquisition blocks, where the so-called noise blocks are recorded. Correlated together, they correspond to the directly detected dimension t_2 of scheme (a). c) Efficient fast acquisition scheme for spin-noise-detected 2D NMR experiments with DBU halves the number of noise block recordings. The mixing and evolution periods and the acquisition block labelled t_0/t_2 are repeated as required to obtain sufficient signal-to-noise ratio. Recycle delays are completely omitted with this scheme, which further reduces the total experimental time.

manded by the nature of the stochastic excitation process. Cross-correlation is achieved as detailed in the paper by Chandra et al.[1] and illustrated in the table of contents graphics. The two noise blocks (t_0 and t_2) are Fourier transformed first and then the resulting spectra are combined by point-wise complex-conjugate multiplication, which owed to the Einstein–Wiener–Khinchin theorem,[16] is equivalent to cross-correlation followed by Fourier transformation. For a 2D experiment this has to be done for each individual point in the indirect time domain t_1 before summation of the repetitions. Fourier transform along t_1 yields the final spin-noise-detected 2D NMR spectrum, which can be phase sensitive in the indirect frequency dimension.

The first actual implementation of the general scheme, the snHMQC experiment[1] is shown in Figure 2a. Even though there are no RF pulses applied on the observed proton (^{1}H) channel, they are still needed on the carbon (^{13}C) channel.

The tiny amplitudes of spin noise signals make it mandatory to repeat the accumulation very often (typically over 1000 times) for each t_1 value. The separation of signals due to coherence transfer from spin noise during t_0 on the one side, and de novo spin noise or random electronic noise in t_2 on the other side, can be achieved because, even though the phases of all contributions are random, the components that undergo coherence transfer via the mixing and evolution periods have constant relative phases in t_0 and t_2. In order to improve the efficiency of spin-noise-detected multi-dimensional NMR our goal was to improve the sensitivity and efficiency (signal-to-noise in a given time interval) of these experiments substantially.

Introducing constant-time evolution (Figure 2b) achieves several improvements. Firstly, constant-time evolution avoids

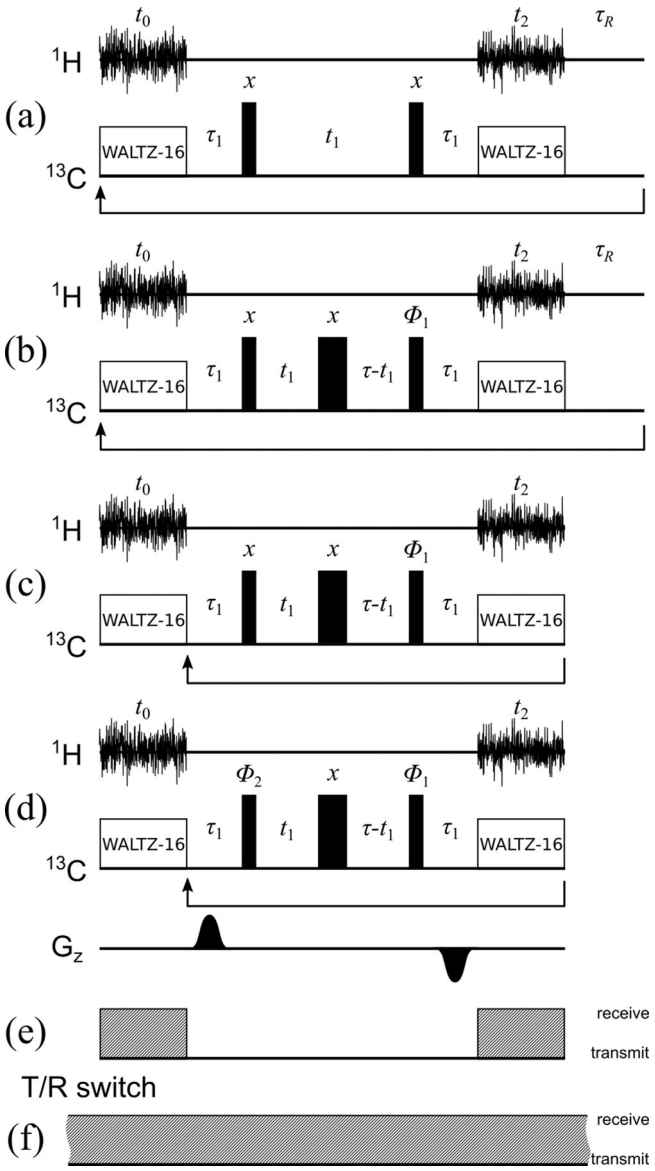

Figure 2. Pulse sequences for the original[1] and enhanced snHMQC and snHMBC experiments. t_0 and t_2 denote the two acquisition blocks. τ_1 is nominally set to $1/(2J_{CH})$ but can be optimized for relaxation and passive couplings (J_{CH} denotes the heteronuclear coupling constant). t_1 is the evolution time (^{13}C). WALTZ-16 decoupling is indicated by the correspondingly labeled blocks. Narrow and wide black rectangles denote hard 90° and 180° RF pulses, respectively. The data collected during the acquisition blocks are stored separately. Panel (a) shows the original snHMQC experiment[1]. Panel (b) shows the pulse sequence for the constant-time ctsnHMQC experiment. The constant time τ is nominally set to $1/J_{CC}$ (J_{CC} denotes the homonuclear carbon coupling constant) but can be optimized for relaxation and competing couplings as given in the Experimental Section. The phase Φ_1 is 0° in the basic sequence. For States-TPPI quadrature detection, first N noise blocks are recorded with $\Phi_1 = 0°$, then with $\Phi_1 = 90°$. Upon each incrementation of t_1, Φ_1 is incremented by 180°. Panel (c) shows the ctsnHMQC experiment with DBU. Panel (d) shows the pulse sequence of the ctsnHMBC experiment. The changes from ctsnHMQC are the addition of z-gradient pulses and the first 90° pulse also having a variable phase Φ_2. Each setting of Φ_1 is recorded with $\Phi_2 = 0°$ and $\Phi_2 = 180°$, while Φ_1 does not apply TPPI anymore (no phase increment per t_1 increment). Panel (e) shows the classical way of switching the preamplifier from transmit to receive mode. Panel (f) shows the new scheme avoiding preamplifier mode switching in order to prevent transmit/receive (T/R) switching artifacts.

the splitting by homonuclear ^{13}C–^{13}C coupling in the indirect dimension, which is relevant when using uniformly ^{13}C labeled samples. The choice of the constant-time interval τ depends on all heteronuclear couplings and relaxation of multiple quantum coherence. It can be optimized to give a maximum in-phase coherence at the end of the evolution period. In practice, the mixing and evolution periods should be kept as short as possible to minimize loss of residual coherence between the first noise block (t_0) and the second one (t_2). Secondly, constant-time evolution provides for quadrature detection in the indirect dimension as outlined later. In the acquisition scheme of Figure 1 with actual pulse sequences shown in Figure 2a and b, noise blocks t_0 and t_2 are recorded separately for each of the N repetitions, yielding N cross-correlated spectra to accumulate for each t_1 value. After each acquisition of a t_2 noise block, there is a recycle delay τ_R, followed by the acquisition of the t_0 noise block of the next repetition. As, relying on spin noise, there is no need to wait for any spin system recovery, one can skip the recycle delay within spectrometer system's timing requirements. With data acquired in this way, during processing every noise block (except the first and last one) can be used as a t_2 block for one and as a t_0 block for the subsequent cross-correlation computation.

This effectively means repeating the basic sequence ("noise acquisition–mixing–evolution–mixing") without delay (Figure 1c), a fast acquisition scheme we denote "double block usage" (DBU). Any magnetization coherently transferred between t_0 and t_2, that has not fully decayed by the end of one t_2 acquisition block, will undergo another "mixing–evolution–mixing sequence" until it decays below any reasonable detection limit. Conversely, the de novo spin noise originating during the t_2 period will cross-correlate with the next noise block as before. With the original scheme (Figure 1b), N recorded noise blocks yield $N/2$ cross-correlations. The DBU scheme increases this number to $N-1$. For larger N the number of cross-correlations thus is practically increased by a factor of two. As the accumulated spin noise signal increases linearly with the number N of cross-correlated spectra added, while the background noise only increases with the $\sqrt{N}$, this results in a factor $\sqrt{2}$ improvement of the signal-to-noise ratio over the original approach.[1] Additionally, the elimination of the recycle delays reduces the total experiment time further.

We implemented DBU in the ctsnHMQC (constant-time snHMQC) experiment also adding quadrature detection in the indirect dimension using the States-TPPI (time-proportional phase incrementation[17,18]) approach, by varying the phase Φ_1 accordingly, as shown in Figure 2c. Thus signals, which are not modulated during t_1 are moved to the edge of the spectrum. The phase sensitive detection enables one to combine parallel coherence transfer pathways to yield a single peak (as opposed to the double and zero quantum coherence cross peaks ($\Omega_H \pm \Omega_C$) of the original experiment) so that another $\sqrt{2}$ sensitivity improvement is achieved.

In the long-range correlation experiment (ctsnHMBC, Figure 2d) we use additional pulsed field gradients during the mixing periods, which is due to the following rational: During the τ_1 period the ^1H transverse magnetization coupled to ^{13}C evolves into antiphase coherence. The pulsed field gradient during this period spatially disperses transverse magnetization thus reducing the amount or radiation damping,[19] which would otherwise quench the signal available for cross-correlation. A gradient of opposite sign in the next τ_1 period refocuses only these coherences, while others, which would enhance radiation damping, are dispersed. The introduction of the pulsed field gradients thus improves the signal-to-noise ratio especially for long mixing times. Apart from counteracting radiation damping, the sign alternating gradient pulses defocus potential signals originating from noise originating between the detection periods. These would contribute to the uncorrelated noise in the spectrum and thus reduce its signal-to-noise ratio. It should be noted that, when using gradients with the fast DBU technique, the fast repetition of gradient may prevent the operation of the spectrometer's field-frequency lock. To mitigate this interference, extra delays between incrementations of t_1 may be required to allow for magnetic field re-optimization. Their duration is however negligible compared to the total experiment time. The states scheme for quadrature detection is used for the ctsnHMBC experiment, too. However, TPPI is replaced by a simple axial peak suppression scheme using 0°/180° alternating phase for Φ_2 (on the first 90° pulse) and subtraction of the resulting spectra (after 1D FT, correlation and summation) during processing so the correlated signals add up constructively. Thus, for each t_1 value, there are four sets of repetitions (instead of two used in ctsnHMQC) alternating Φ_1 between 0° and 90° and Φ_2 between 0° and 180° independently. It should be noted that in this type of experiment each phase cycling step has to be stored separately as is also the case in multiplex NMR methods.[20]

While testing spin-noise-detected experiments on different spectrometers we noticed evidence of spurious excitation on some hardware configurations. The experiments documenting that behavior are laid out in the Supporting Information. In summary, the active impedance switching of the preamplifier between a low impedance (50 Ω) "pulse mode" and a high impedance "receive mode" can cause minute signal excitation of random phase and amplitude occurring at the moment of activation of this transmit/receive (T/R) switch. The common T/R switching scheme implemented in the standard acquisition schemes can be seen in Figure 2e. To avoid any influence of impedance switching all new experiments shown here were using new implementations of the pulse programs explicitly programming the T/R switch to remain in receive mode all the time, which is shown in Figure 2f. The pulse programs are available in the Supporting Information.

In Figure 3 we compare the first spin-noise-detected 2D NMR spectrum[1] to the improved version (ctsnHMQC, Figure 2c) with all improvements outlined above applied.

Even though the total recording time was shrunk from the original 40 h to just 20 h, the signal-to-noise ratio could be improved by a factor of approximately $\sqrt{2}$. This is owed to the combined effects of the DBU and phase sensitive quadrature detection both contributing a factor of approximately $\sqrt{2}$. Additionally, the faster recycle time and lower requirement of long-term stability as well as the elimination of spurious excita-

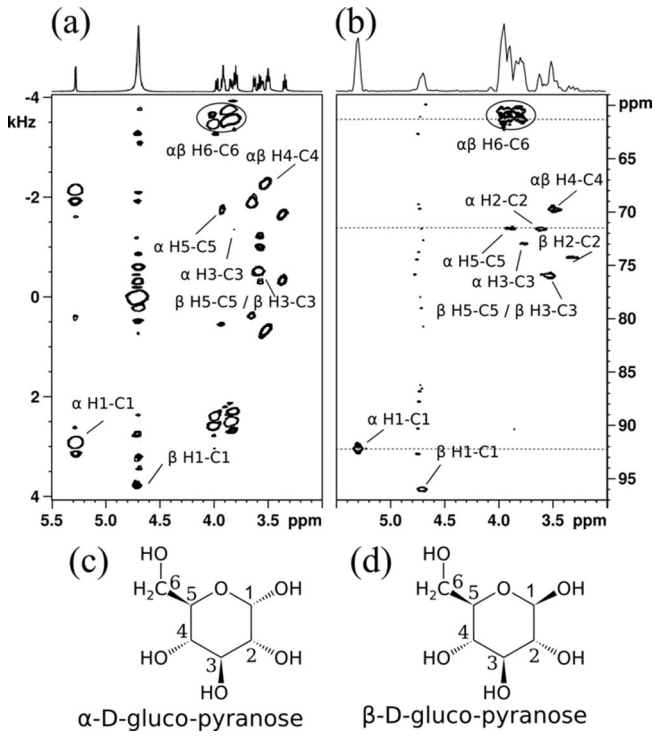

Figure 3. Panel (a) depicts the first 2D spin-noise-detected (snHMQC) spectrum published by Chandra et al.[1] (recording time: 40 h). The 1D trace is a standard ^{1}H spectrum. In panel (b), we show the result of the current implementation of the ctsnHMQC experiment according to Figure 2c and e applying all enhancements laid out in the text. Total recording time was 20 h. Note the absence of the zero quantum ($\Omega_H - \Omega_C$) peaks in panel (b). The 1D spectrum is a projection of the 2D spectrum. Horizontal dashed lines mark the locations of the cross sections shown in Figure 4. The numbering of the prevailing isomers of glucose in aqueous solution is shown in panel (c) for the α-D-pyranose and in panel (d) for the corresponding β anomer.

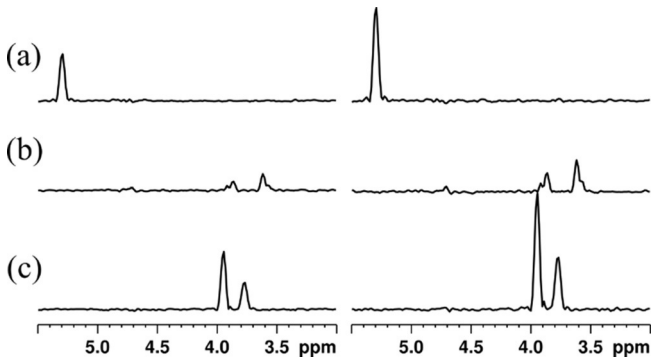

Figure 4. ^{1}H cross sections from ctsnHMQC spectra obtained from the same raw data as Figure 3b. Traces on the left are processed without DBU, whereas traces on the right are processed using DBU. Traces (a) were taken from the corresponding 2D spectra at 61.4 ppm, trace (b) at 71.5 ppm, and trace (c) at 92.2 ppm as indicated in Figure 3b.

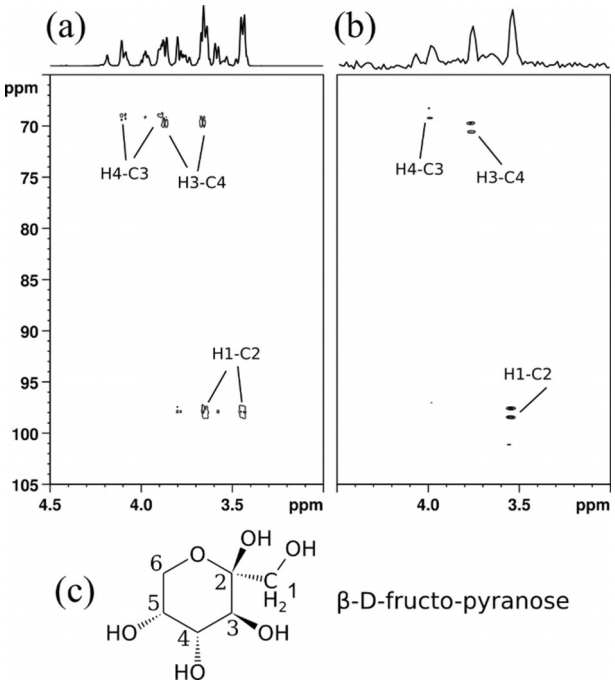

Figure 5. Pulsed and noise-detected HMBC experiments of D-fructose. The spectrum in panel (a) was obtained using a standard pulsed HMBC experiment (pulse program: 'hmbcgpndqf')[23] and is compared to the results of the ctsnHMBC experiment in panel (b). The recording time of the ctsnHMBC was 80 h; resolution(F1) = 22.0 Hz; resolution(F2) = 19.1 Hz. Panel (c) shows the numbering of the most abundant fructose isomer in aqueous solution.

tion background, the improvement exceeds the theoretical factor of 2 slightly. All single bond hydrogen-carbon coupling pairs of both anomeric forms of the gluco-pyranose could be identified in the new faster and more sensitive version of the experiment. It is also noteworthy, that due to the improvements of the recording technique, the t_1 noise artifacts visible at 4.7 ppm (from residual HOD) in Figure 3a are absent from the improved spectrum of Figure 3b.

In Figure 4 we illustrate the gain in signal-to-noise ratio obtained through the DBU scheme by comparing three cross sections obtained from the same raw data as Figure 3b. The traces on the left side were obtained without DBU. The spin noise signal power amplitudes in the right side traces are approximately doubled owed to the use of DBU. As the uncorrelated noise power also increases by a factor $\sqrt{2}$ the signal-to-noise ratio rises by $\sqrt{2}$, too.

Taking advantage of the improved sensitivity a heteronuclear long-range correlation experiment (HMBC)[21,22] was implemented in a spin-noise-detected fashion, ctsnHMBC. In Figure 5 the results of the first implementation of a ctsnHMBC experiment are compared with a standard pulsed HMBC experiment. While demonstrating a new breakthrough in spin-noise-detected NMR, the experiment clearly shows up its current limits, as only the two correlations, for which the chosen mixing delays match best can be unequivocally identified. The H4–C3 correlation, for example, is not detected due to insufficient signal-to-noise ratio.

Overall, the concept of two-dimensional spin noise NMR spectroscopy could be extended significantly. The experimental schemes of spin-noise-detected 2D NMR were substantially improved and adapted to avoid an artifact present on some spectrometer hardware, which is related to the active switching between a transmit and a receive state in the preamplifier

electronics. This insight appears to be important, because this interference may influence the outcome of spin noise experiments drastically. Notably, it may increase the amount of uncorrelated noise background in the experiments relying upon cross-correlation to distinguish between completely random and coherently transferred spin noise components.

We have shown that standard protocols of pulsed NMR, like phase cycling, pulsed field gradients and States or TPPI schemes can be used to improve the signal-to-noise ratio, achieve quadrature detection in the indirect dimension, and remove artifacts. These results demonstrate that many "tools of the trade" of traditional NMR can be applied for spin-noise-detected NMR spectroscopy.

The DBU fast acquisition scheme introduced here represents a paramount and unique acceleration of spin noise spectroscopy, because it achieves a tremendous speedup of the experiments, which is not possible in pulsed excitation NMR due to the dependence on longitudinal relaxation. Comparing the original experiment[1] at equal recording times and on identical hardware, we have been able to achieve an increase by nearly a factor of three in signal-to-noise ratio by combining all improvements described here, which boils down to nearly one order of magnitude in experimental time. While the real benefit of this will only be of practical relevance, once a future "nano-NMR spectrometer" is constructed, stochastic NMR excitation techniques using an RF noise source may also take advantage from the DBU principle.[24] The DBU acceleration principle for coherent spectroscopic techniques is not limited to Faraday detection as in the application outlined here, it is likewise suitable to be incorporated in optical detection methods, as for example in the novel nano-scale NMR detected indirectly by NV-centers in diamonds.[25]

Experimental Section

The substances used for demonstrating the spin noise NMR experiments were uniformly 99 at.% ^{13}C enriched D-glucose (Aldrich) for all HMQC-type experiments and 99 at.% ^{13}C enriched D-fructose (Aldrich) for all HMBC-type experiments. The solvent was D_2O (Euriso-Top, 99.90 at.% D). The concentration was 0.65 mol L^{-1} for the D-glucose (as in the original experiment[1]) and 3.20 mol L^{-1} for D-fructose. We note that spin-noise-detected experiments involving coherence transfer are best conducted in the regime of positive spin noise signal[8,26] to mitigate quenching by radiation damping. The validity of this condition was tested before the 2D experiments by recording one dimensional spin noise spectra.

The effectiveness of the cross-correlation processing is critically affected by transverse relaxation between the respective noise blocks, which was taken care of through optimization of the delay times in the pulse sequences as given below. This optimization was effected by prepending a single 1 μs ^1H pulse to a train of 32 repetitions of the respective pulse sequence and maximizing cross peak intensities in the spectra processed identically to the spin noise spectra. The apparent fast transverse relaxation rates under the conditions given (e.g. $T_2^* \cong 10\ s^{-1}$ for the anomeric protons) are mostly owed to radiation damping, which can be suppressed during the coupling precession intervals τ_1 by application of sign alternating pulsed field gradients.

Standard (Wilmad 535) 5 mm NMR sample tubes were used. Spectra were recorded at 313 K on a 700 MHz Bruker Avance III spectrometer with a cryogenically cooled TCI triple resonance (H,C,N,D) probe manufactured in 2011. Common parameters for both spectra in Figure 3 were duration of acquisition $t_0 = t_2 = 26.2$ ms corresponding to a resolution of 19.1 Hz in F2; t_1 increments were adjusted for a spectral width of 7044.5 Hz (40 ppm) in F1 and the maximum duration of t_1 was set to 22.7 ms corresponding to a resolution of 22.0 Hz in F1; $\tau_1 = 3.45$ ms and $\tau = 22.7$ ms. For the ctsnHMBC experiment of Figure 5c the pulse sequence of Figure 2d with $\tau_1 = 55.6$ ms; $\tau = 22.7$ ms and shaped (squared sine bell) pulsed field gradients with 2% of the full amplitude (50 Tm^{-1}) and 5 ms duration were used.

To mitigate long-term instability (temperature, humidity, vibrations, etc.) of the spectrometer environment in general, all the experiments were recorded in multiple sections, which were combined during processing. Acquisition of each section lasted approx. 2 h and in between the recording of individual sections magnetic field corrections (Bruker's "topshim" procedure) were re-optimized. For example, for an experiment with a total duration of 20 h, ten full 2D experiments were recorded each lasting for about 2 h and finally combined. The increase in total recording time due to periodic automated shimming is less than 5%. The script for the automatic acquisition and shimming sequence is shown in the Supporting Information.

Acknowledgements

The research reported was supported in part by the Austrian Science Funds FWF (Project M1404 for K.C. and N.M. and Project I1115-N19 for N.M.), as well as by the European Union through the ERDF INTERREG IV (RU2-EU-124/100–2010) program (Project M00146, "RERI-uasb" for N.M.). Inspiring discussions with members of the COST (European Cooperation in Science and Technology) Action CA15209 EURELAX are acknowledged. We are grateful to Dr. Wolfgang Bermel (Bruker-BioSpin, Germany) for support in programming within the TopSpin environment.

Conflict of interest

The authors declare no conflict of interest.

Keywords: cross-correlation · fast acquisition · multiple-quantum coherence · nuclear spin noise · two-dimensional nuclear magnetic resonance

[1] K. Chandra, J. Schlagnitweit, C. Wohlschlager, A. Jerschow, N. Müller, *J. Phys. Chem. Lett.* **2013**, *4*, 3853–3856.
[2] F. Bloch, *Phys. Rev.* **1946**, *70*, 460–474.
[3] T. Sleator, E. L. Hahn, C. Hilbert, J. Clarke, *Phys. Rev. Lett.* **1985**, *55*, 1742–1745.
[4] M. A. McCoy, R. R. Ernst, *Chem. Phys. Lett.* **1989**, *159*, 587–593.
[5] H. Kovacs, D. Moskau, M. Spraul, *Prog. Nucl. Magn. Reson. Spectrosc.* **2005**, *46*, 131–155.
[6] M. Guéron, J. L. Leroy, *J. Magn. Reson.* **1989**, *85*, 209–215.
[7] N. Müller, A. Jerschow, *Proc. Natl. Acad. Sci. USA* **2006**, *103*, 6790–6792.
[8] M. T. Pöschko, V. V. Rodin, J. Schlagnitweit, N. Müller, H. Desvaux, *Nat. Commun.* **2017**, *8*, 13914.
[9] J. Schlagnitweit, N. Müller, *J. Magn. Reson.* **2012**, *224*, 78–81.
[10] M. Bechmann, N. Müller, *Annu. Rep. NMR Spectrosc.* **2017**, *92*, 199–226.

[11] M. T. Pöschko, B. Vuichoud, J. Milani, A. Bornet, M. Bechmann, G. Bodenhausen, S. Jannin, N. Müller, *ChemPhysChem* **2015**, *16*, 3859 – 3864.
[12] M. Nausner, J. Schlagnitweit, V. Smrečki, X. Yang, A. Jerschow, N. Müller, *J. Magn. Reson.* **2009**, *198*, 73 – 79.
[13] N. Müller, A. Jerschow, J. Schlagnitweit, *eMagRes* **2013**, *2*, 237 – 243..
[14] C. L. Degen, M. Poggio, H. J. Mamin, C. T. Rettner, D. Rugar, *Proc. Natl. Acad. Sci. USA* **2009**, *106*, 1313 – 1317.
[15] W. P. Aue, E. Bartholdi, R. R. Ernst, *J. Chem. Phys.* **1976**, *64*, 2229 – 2246.
[16] A. Einstein, *Arch. Sci. Phys. Nat.* **1914**, *37*, 254 – 256; N. Wiener, *Acta Math.* **1930**, *55*, 117 – 258; A. Khintchine, *Mathem. Annal.* **1934**, *109*, 604 – 615.
[17] D. J. States, R. A. Haberkorn, D. J. Ruben, *J. Magn. Reson.* **1982**, *48*, 286 – 292.
[18] D. Marion, K. Wüthrich, *Biochem. Biophys. Res. Commun.* **1983**, *113*, 967 – 974.
[19] V. Sklenar, *J. Magn. Reson.* **1995**, *114*, 132 – 135.
[20] J. Schlagnitweit, M. Hornicakova, G. Zuckerstätter, N. Müller, *ChemPhysChem* **2012**, *13*, 342 – 346.
[21] W. Schöfberger, J. Schlagnitweit, N. Müller, *Annu. Rep. NMR Spectrosc.* **2011**, *72*, 1 – 60.
[22] A. Bax, M. F. Summers, *J. Am. Chem. Soc.* **1986**, *108*, 2093 – 2094.
[23] TopSpin v3.5pl5, Bruker-Biospin, Rheinstetten, Germany **2016**.
[24] B. Blümich, *J. Magn. Reson.* **1990**, *90*, 535 – 543.
[25] N. Aslam, M. Pfender, P. Neumann, R. Reuter, A. Zappe, F. Fávaro de Oliveira, A. Denisenko, H. Sumiya, S. Onoda, J. Isoya, J. Wrachtrup, *Science* **2017**, *357*, 67 – 71.
[26] P. Giraudeau, N. Müller, A. Jerschow, L. Frydman, *Chem. Phys. Lett.* **2010**, *489*, 107 – 112.

Manuscript received: January 3, 2018
Accepted manuscript online: February 4, 2018
Version of record online: February 20, 2018

